# Novel measurements of refractive index, density and mid-infrared integrated band strengths for solid $O_2$, $N_2O$ and $NO_2$:$N_2O_4$ mixtures

D. Fulvio [a,b,*], B. Sivaraman [c], G.A. Baratta [b], M.E. Palumbo [b], N.J. Mason [c]

[a] Department of Physics & Astronomy, Catania University, Via S. Sofia 64, I-95123 Catania, Italy
[b] INAF – Catania Astrophysical Observatory, via S. Sofia 78, I-95123 Catania, Italy
[c] Department of Physics & Astronomy, The Open University, Walton Hall, Milton Keynes MK7 6AA, United Kingdom

## ARTICLE INFO

## ABSTRACT

We present novel measurements of the refractive index, density and integrated band strengths of mid-infrared features of solid $N_2O$ at 16 K and of $NO_2$ and $N_2O_4$ in two frozen $NO_2$:$N_2O_4$ mixtures deposited at 16 and 60 K. The refractive index and density measurements were performed also for frozen $O_2$ deposited at 16 K. In this case, the integrated band strength values could not be determined since $O_2$ is a homonuclear molecule and therefore its fundamental mode is not infrared active. The solid samples were analysed by infrared spectroscopy in the 8000÷800 cm$^{-1}$ range. The sample thickness was measured by the interference curve obtained using a He–Ne laser operating at 543 nm. The refractive index at this laser wavelength was obtained, by numerical methods, from the measured amplitude of the interference curve. The density values were obtained using the Lorentz–Lorenz relation. Integrated band strength values were then obtained by a linear fit of the integrated band intensities plotted versus column density values. The astrophysical relevance of these novel measurements is briefly discussed.

## 1. Introduction

N–O containing molecules, such as NO, HNO, $N_2O$, have been detected in the gas phase both in low-mass and high-mass star-forming regions [1–5] though the role of nitrogen chemistry in interstellar chemistry remains largely not understood. Since astronomical observations indicate that in dense molecular interstellar regions gas phase species freeze out on dust grains and form "icy" grain mantles [6–8], it is likely that some of these species exist even in the condensed phase. Furthermore, dust grains present in these environments suffer from the effects of cosmic ion irradiation and UV photolysis [9–11]. Solar System observations have shown that the surface of the outer planets and satellites as well as comets and asteroids are rich of several simple molecules such as CO, $N_2$, $CH_4$, $H_2O$ in solid form (e.g., [12] and [13]). These bodies are continuously irradiated by solar energetic ions and galactic cosmic rays [14].

Laboratory experiments have shown that N–O bearing molecules are easily formed after ion and UV irradiation of C- and N- bearing frozen gas mixtures such as CO:$N_2$ mixtures in the solid form ([15], Palumbo et al., in preparation). Thus it is reasonable to expect that N–O bearing species are present in the solid phase both on the surface of external bodies in the Solar System (such as Pluto and Triton) and within interstellar "icy" mantles even if these have not yet been detected.

However, in order to estimate the abundance of such species both in astronomical spectra and laboratory spectra integrated band strengths (often referred to as A values) are required and, to date, experimental measurements of A values for the solid phase of $N_2O$ and $NO_2$ are missing.

Oxygen is the most abundant element in the Universe after hydrogen and helium and therefore it is expected to be present in the solid phase in "icy" grain mantles and an upper limit for its abundance has been estimated [16]. Observations in the 0.24÷5.2 μm spectral range indicate the presence of frozen molecular oxygen on the surface of Solar System objects such as the Jovian moon Ganimede [17].

Nitrogen dioxide ($NO_2$) and nitrous oxide ($N_2O$) are also present in Earth's atmosphere. These two species occur both in stratosphere and troposphere [18–21] and, in particular, $N_2O$ is one of the main greenhouse gas and biomarker species, being released into the atmosphere mainly by biological sources [22 and references therein].

In this paper, we present novel measurements of refractive index, density and integrated band strengths of mid-infrared features for solid $N_2O$ at 16 K and for $NO_2$ and $N_2O_4$ in two frozen $NO_2$:$N_2O_4$ mixtures deposited at 16 and 60 K, respectively. We also report refractive index and density measurements for frozen $O_2$

* Corresponding author at: INAF – Catania Astrophysical Observatory, via S. Sofia 78, I-95123 Catania, Italy. Tel.: +39 095 7332325; fax: +39 095 330592.
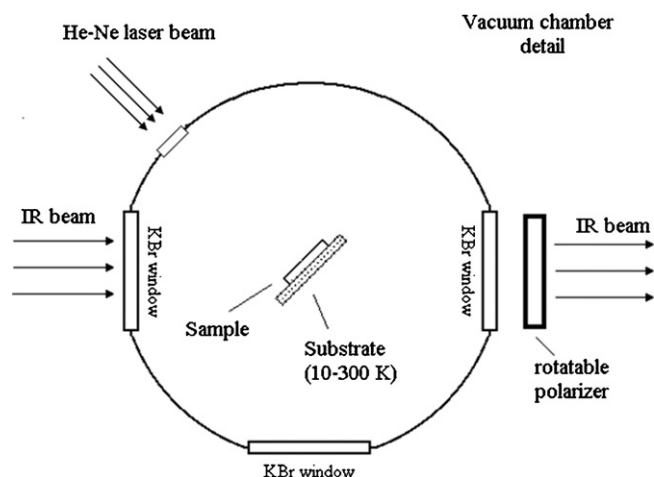E-mail address: dfu@oact.inaf.it (D. Fulvio).

**Fig. 1.** Schematic view of the experimental apparatus.

**Table 1**
Values of density and refractive index measured for solid $O_2$, $N_2O$ and $NO_2$ deposited at 16 K on a Si substrate. For frozen $NO_2$ these quantities are also measured at 60 K.

| Molecule | Temperature (K) | Density (g cm$^{-3}$) | Refractive index |
|---|---|---|---|
| $O_2$ | 16 | 1.54 | 1.322 |
| $N_2O$ | 16 | 1.16 | 1.318 |
| $NO_2$ | 16 | 1.17 | 1.316 |
| $NO_2$ | 60 | 1.90 | 1.548 |

**Table 2**
Values of density and refractive index used to calculate, by means of Eq. (1), the $L$ value of the molecular species considered in this work. The related material phase and temperature is also reported.

| Molecule | Phase | Temperature (K) | Density (g cm$^{-3}$) | Refractive index |
|---|---|---|---|---|
| $O_2$ | Solid | 20 | 1.22 | 1.25 [25] |
| $N_2O$ | Solid | 20 | 0.99 | 1.27 [25] |
| $NO_2$ | Liquid | 300 | 1.45 | 1.40 |

deposited at 16 K. In this case, integrated band strength values could not be determined since $O_2$ is a homonuclear molecule so its fundamental mode is not infrared active. The present measurements will allow us to calculate the column densities (i.e. the abundance in molecules/cm$^2$) of these molecules in observed mid-infrared spectra in both the astrophysical and terrestrial environments in which they occur.

## 2. Experimental apparatus

The present experiments were performed in the Laboratory for Experimental Astrophysics in Catania (Italy). The experimental apparatus used to obtain infrared transmission spectra of pure frozen $O_2$ and $N_2O$ (at 16 K) and $NO_2$:$N_2O_4$ frozen mixtures (at 16 and 60 K) of different thicknesses, in the range 8000÷800 cm$^{-1}$, is shown schematically in Fig. 1. It is composed of a stainless steel high-vacuum chamber operating at a pressure $P < 10^{-7}$ mbar interfaced to a FTIR spectrophotometer (Bruker Vertex 70) through IR-transparent windows. Frozen species are accreted by a gas inlet onto a chosen substrate (in our case Si or KBr) inclined at an angle of 45° with respect to the infrared beam. The substrate is placed in thermal contact with a closed-cycle helium cryostat whose temperature can be varied in the 10–300 K range (see [23] for further

details). With this experimental set-up we can monitor the thickness of the film during its accretion on the substrate by looking at the interference pattern (intensity versus time) given by a He–Ne laser beam (543 nm) reflected at near normal incidence (2.9°) by the vacuum–solid and solid–substrate interfaces. After the reflection from the substrate, the laser beam is detected by using an external silicon-diode detector. For each selected thickness, two spectra are taken, one with the electric vector parallel (P polarized) and one perpendicular (S polarized) to the plane of incidence. The polarization is set using a rotatable polarizer placed in the path of the infrared beam. All the spectra were taken with a resolution of 1 cm$^{-1}$.

## 3. Results

### 3.1. Refractive index and density

To calculate the thickness of the species deposited on the silicon substrate it is necessary to determine the optical properties of the frozen film. The refractive index of the condensed film is the key parameter if we are to measure its density and thickness. In general the interference curve versus thickness is an oscillating function and for absorbing materials, the laser light transmitted into the film and reflected back by the interface film–substrate is attenuated in the film. The amplitude of the oscillation in the interference
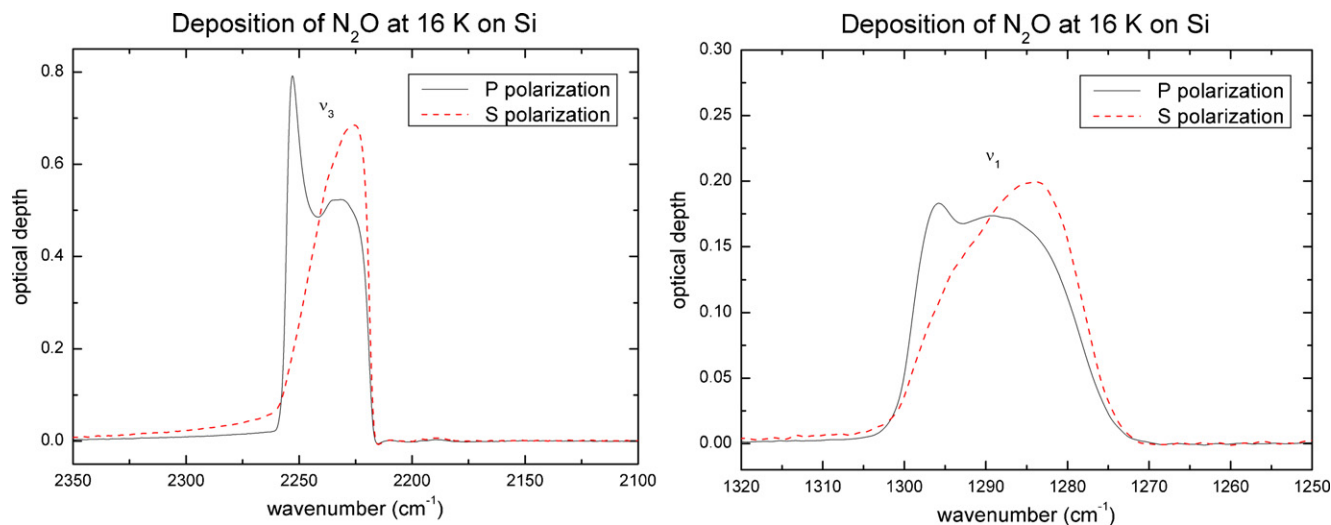


**Fig. 2.** Comparison between the profile of the $\nu_1$ (1295 cm$^{-1}$) and $\nu_3$ (2239 cm$^{-1}$) mid-infrared features of frozen $N_2O$ deposited on a Si substrate at 16 K in P and S polarization. The bands in P polarized spectra show an additional feature due to longitudinal modes.

curve exponentially decays with the thickness, and the reflectance approaches its bulk value at a large thickness. Anyway, in molecular frozen solids probed by visible light, the absorption is so low that it can be neglected for a thickness of a few micrometers (as in this work).

In particular, the amplitude of the experimental interference curve depends on the refractive index $n_f$ of the species at laser wavelength (543 nm), the refractive index $n_s$ of the substrate, the incidence angle $\theta_i$ of the laser beam and on the polarization of the laser light. Hence, being all the other quantities known, $n_f$ can be derived, using numerical methods, from the measured amplitude of the experimental interference curve (intensity ratio between maxima and minima). The refractive index values obtained in this work are listed in Table 1.

From the derived $n_f$ value, we can also estimate the film density using the Lorentz–Lorenz relation. In particular, for a given species the Lorentz–Lorenz coefficient, $L$, is nearly constant for a fixed wavelength regardless of the material phase and temperature [24]. This quantity is related to the density by the Lorentz–Lorenz relation:

$$L\rho = \frac{n_f^2 - 1}{n_f^2 + 2} \tag{1}$$

According to [25], frozen $O_2$ at 20 K has a density $\rho = 1.22\,\mathrm{g\,cm^{-3}}$ and a refractive index of $n_f = 1.25$. The corresponding Lorentz–Lorenz coefficient is equal to $0.1294\,\mathrm{cm^3\,g^{-1}}$ at $\lambda = 632.8$ nm. Although $L$ is a function of wavelength through the refractive index, we can neglect, for a material transparent in the visible, the variation of the refractive index between 543 and 632.8 nm. Hence, to a first approximation, we can assume that the $L$ coefficient does not vary between 543 and 632.8 nm. By substituting this $L$ value in Eq. (1) and the value of the refractive index measured by interference, we obtain for our experimental deposition conditions a density $\rho = 1.54\,\mathrm{g\,cm^{-3}}$ for frozen $O_2$ at 16 K. Similarly, by using the $n$ and $\rho$ values for solid $N_2O$ measured by [25] (see Table 2), we obtain a density $\rho = 1.16\,\mathrm{g\,cm^{-3}}$ for frozen $N_2O$ at 16 K. In the case of $NO_2$, we used the density and refractive index available from commercial catalogues for the liquid phase in order to derive the Lorentz–Lorenz coefficient. By using this $L$ value we obtain a density of $\rho = 1.17\,\mathrm{g\,cm^{-3}}$ and $\rho = 1.90\,\mathrm{g\,cm^{-3}}$ for frozen $NO_2$ deposited at 16 and 60 K, respectively. The $\rho$ values found for the frozen species treated in this work are reported in Table 1.

Once $n_f$ has been derived, we can also measure the thickness of the deposited film by comparing the theoretical interference curve with the experimental one. In particular the period of the interference curve (distance between two maxima or minima) is given by the relation:

$$\Delta d = \frac{\lambda_0}{2n_f\sqrt{1 - \sin^2\theta_i/n_f^2}} \tag{2}$$

where $\lambda_0$ is the laser wavelength and $\theta_i$ the incidence angle. Further details on the method used to derive the refractive index and the thickness can be found in [23] and [26]. The absolute accuracy of the thickness measured in this way is about 5% and it is mainly limited by the uncertainties in the knowledge of the refractive index of the Si substrate at low temperature and by the error in measuring the incidence angle of the laser.

### 3.2. Band strengths

Using the values of thickness $d$ (cm) and density $\rho$ ($\mathrm{g\,cm^{-3}}$) calculated above, we can derive the column density $N$ (molecules $\mathrm{cm^{-2}}$) for a species of molecular weight $\mu$ (g) using the following
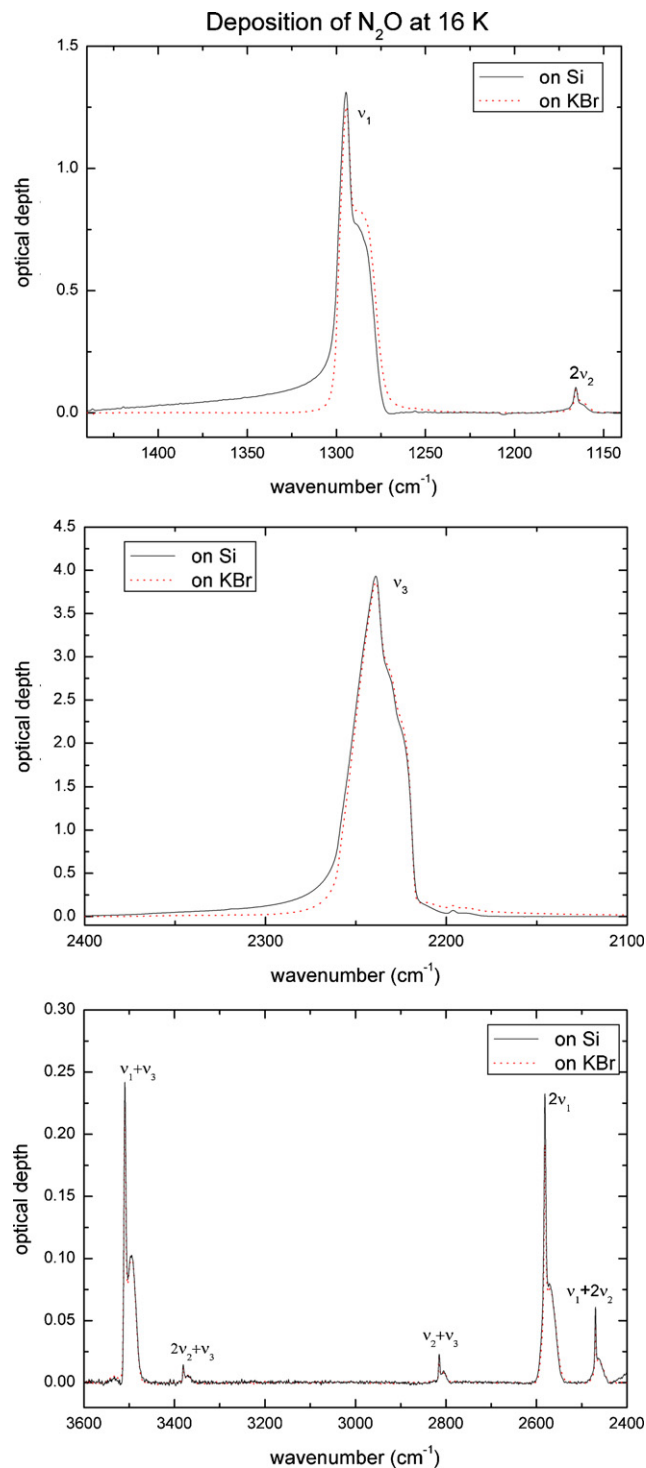


**Fig. 3.** IR spectra (in three different spectral regions) of frozen $N_2O$ deposited at 16 K on KBr and Si substrate. The y-scale is different for the sake of clarity.

relation:

$$N = \frac{d\rho}{\mu} \tag{3}$$

From the infrared spectra, the integrated intensity (area) of a selected band (in optical depth $\tau(\nu)$ scale) is measured for different film thicknesses in order to derive the related integrated band

**Table 3**
Peak position of the IR bands of solid $N_2O$ deposited at 16 K and their assignment [22,29,30].

| Wavenumber (cm$^{-1}$) | Mode |
|---|---|
| 1166 | $2\nu_2$ |
| 1295 | $\nu_1$ |
| 2239 | $\nu_3$ |
| 2469 | $\nu_1 + 2\nu_2$ |
| 2581 | $2\nu_1$ |
| 2814 | $\nu_2 + \nu_3$ |
| 3380 | $2\nu_2 + \nu_3$ |
| 3509 | $\nu_1 + \nu_3$ |

**Table 4**
Peak positions and integrated band strengths for the three most intense features of frozen $N_2O$ deposited at 16 K on two different substrates (Si and KBr).

| Substrate:<br>Peak position (cm$^{-1}$) | Si<br>$A$ (cm molecule$^{-1}$) | KBr<br>$A$ (cm molecule$^{-1}$) |
|---|---|---|
| 2239 | $6.55 \times 10^{-17}$ | $5.69 \times 10^{-17}$ |
| 1295 | $1.22 \times 10^{-17}$ | $1.07 \times 10^{-17}$ |
| 2581 | $1.63 \times 10^{-18}$ | $1.5 \times 10^{-18}$ |

strength $A$ (cm molecule$^{-1}$) value:

$$A = \frac{\int \tau(\nu)d\nu}{N} \qquad (4)$$

It has been shown [23,27,28] that when the band profiles recorded using P and S polarization are similar, the transitions are weak and the features seen in the transmission spectra directly reflect variation of the absorption coefficient of the solid sample. These circumstances have been observed in the frozen $NO_2$:$N_2O_4$ mixture at 16 K, in which case the band strengths have been calculated by using the P polarized spectra since the signal to noise ratio is higher for this polarization. On the other hand, in the case of the frozen $NO_2$:$N_2O_4$ mixture at 60 K and $N_2O$ at 16 K, some absorption features have different profiles in P and S polarizations. This is clearly seen in Fig. 2, where we show the profile of the two main features of frozen $N_2O$ ($\nu_1$ and $\nu_3$) deposited on a Si substrate at 16 K (film thickness = 0.213 µm) in both P and S polarization. In this case the bands in P polarized spectra show an additional feature overlapped (in the left hand side) to that present in S polarized spectra. These additional bands do not correspond to maximum of the absorption coefficient but to longitudinal modes. For this reason, in the case of the frozen $NO_2$:$N_2O_4$ mixture at 60 K and $N_2O$ at 16 K we used S polarized spectra in order to derive the integrated band strengths (e.g., [27]).

Finally we want to point out that column densities and band strengths were derived after correcting the thickness by a factor (from the Snell's low) of $1/\cos\theta_r = 1/\sqrt{1 - \sin^2\theta_i/n_f^2}$, where $\theta_r$ is the refractive angle. This correction takes into account the increased path length of the IR beam at an oblique incidence of $\theta_i = 45°$. The correction factor was derived by assuming a constant value of the

refractive index with the wavelength. This approximation neglects any variations in the refractive index in the infrared spectral region due to the vibrations and contributions of the electronic transitions to the dispersion from the visible (543 nm) to the infrared.

A plot of the band area against the column densities (see Sections 3.2.1 and 3.2.2) is used to derive the band strength values for the main infrared features of frozen $N_2O$ held at 16 K and of $NO_2$ and $N_2O_4$ in two frozen $NO_2$:$N_2O_4$ mixtures deposited at 16 and 60 K, respectively. Since $O_2$ is a homonuclear molecule its fundamental mode is not infrared active and thus no $A$ value has been determined for this molecule.

*3.2.1. $N_2O$*
$N_2O$ films were prepared using a SIO lecture bottle of $N_2O$. Fig. 3 shows the IR spectra of two frozen samples deposited at 16 K respectively on a Si and a KBr substrate. Each spectrum is plotted on an optical depth ($\tau$) scale using the relation $I = I_0 \cdot e^{-\tau}$ (Beer–Lambert law), where $\tau = \alpha \cdot x$ ($\alpha$ = absorption coefficient; $x$ = path length through the material). However it is well known that this is only an approximation and deviations from this relationship may be as high as 20–30% and depend on the optical properties of the substrate.

The bands present in the spectra of Fig. 3 are identified in Table 3, together with their assignment. The weak band appearing at about 2320 cm$^{-1}$ is probably due to the presence of a $N_2$ contamination inside the lecture bottle. Fig. 4 shows the plots of the band area against the column density. The best-fit of these data is used to derive the A values for the three most intense bands of $N_2O$, in the case of the two different substrates used for the deposition. In the A value computation usually we considered five film thicknesses (up to 1.047 µm) for each band, except for the region of strong absorption (see for instance the 2239 cm$^{-1}$ band) where we used just the three thinner film thicknesses to keep the feature far from the saturation level.
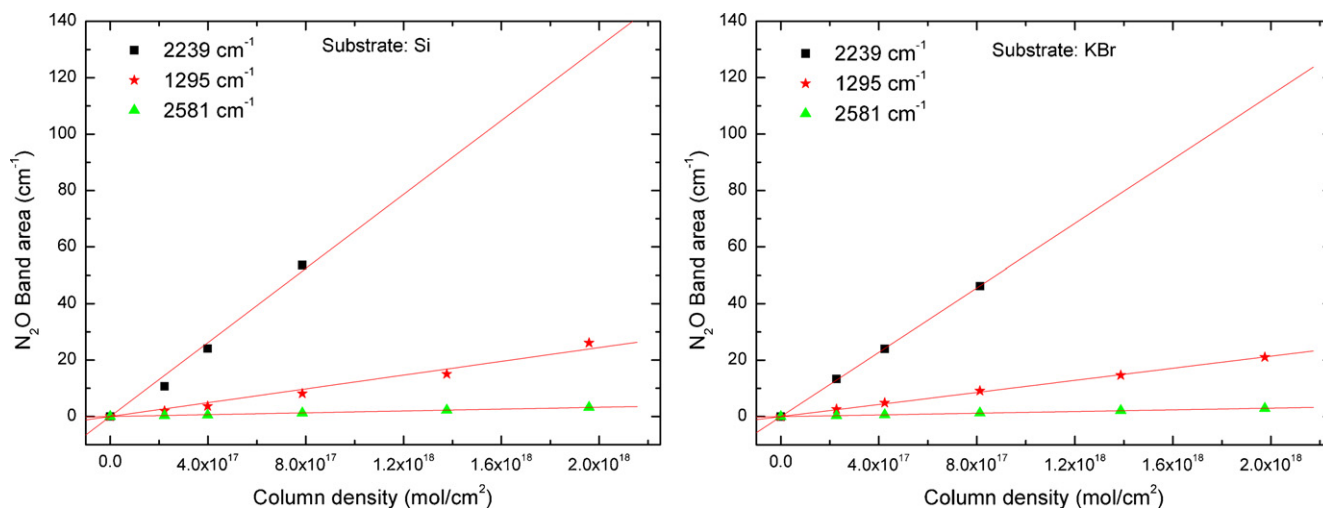


**Fig. 4.** Plot of the band area vs. the column density for the three most intense bands of $N_2O$. The slope of the fit (solid line) gives the value of the integrated band strength A for the corresponding band (see Table 4).
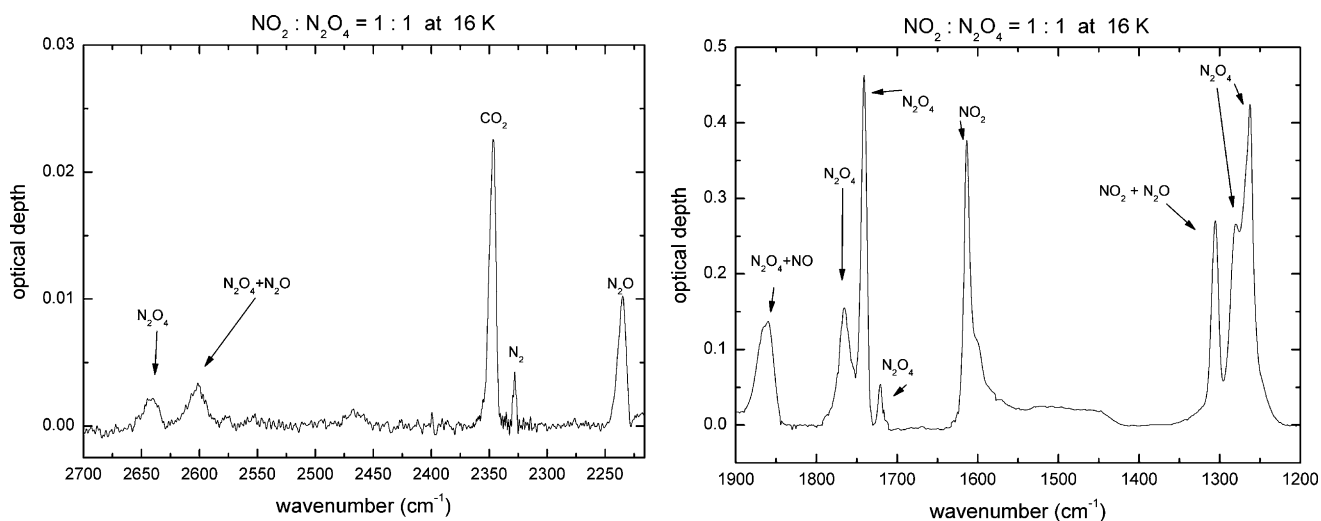
**Fig. 5.** IR spectra (two different spectral regions) of a $NO_2:N_2O_4 = 1:1$ frozen mixture as deposited at 16 K. The y-scale is different for clarity.



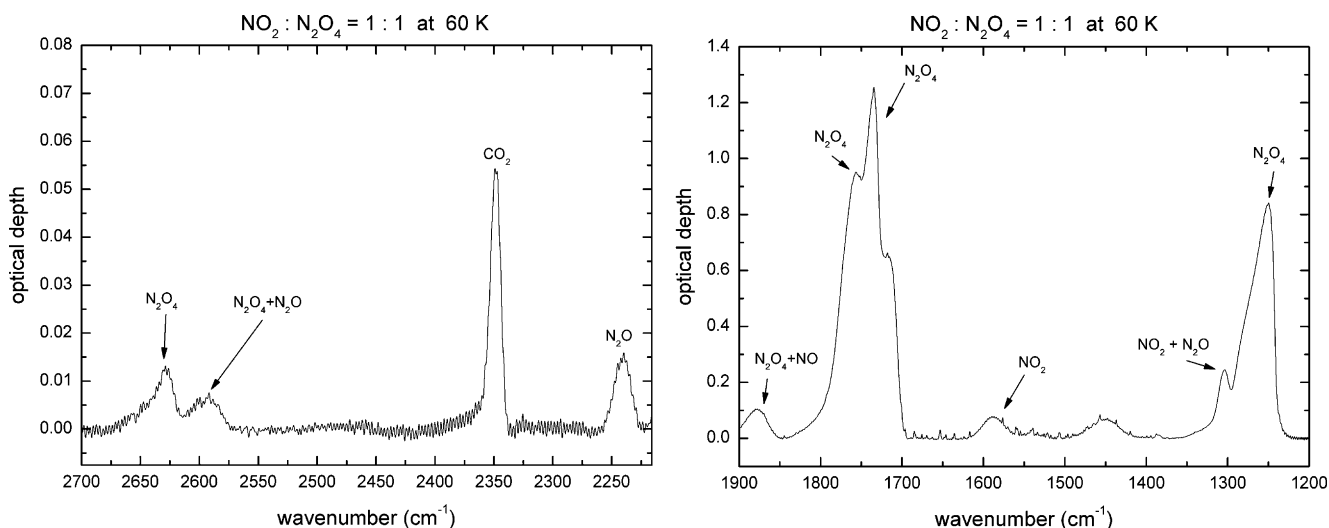**Fig. 6.** IR spectra (same spectral regions of Fig. 5) of a $NO_2:N_2O_4 = 1:1$ frozen mixture as deposited at 60 K. The y-scale is different for clarity.

Table 4 reports the integrated band strength values so estimated. We note that differences due to the substrate in the obtained A values range between 15% and 25%. These differences can be explained by the limits of applicability of the Beer–Lambert law.

### 3.2.2. $NO_2:N_2O_4$ mixtures

$NO_2:N_2O_4$ mixtures were prepared using an Aldrich lecture bottle of $NO_2$ stated to be of $\geq 99.5\%$ purity. Before to reach the vacuum chamber ($P < 10^{-7}$ mbar) the gas is admitted in a pre-chamber, kept at room temperature, at a given pressure. We must point out that $NO_2$ monomer is in equilibrium with its own $N_2O_4$ dimer so dimers are always present with $NO_2$. Therefore, to know what mixture $NO_2:N_2O_4$ we are depositing on the substrate, we need to determine the relative concentration of these two species within our experimental set up.

For the association–dissociation reaction $2NO_2 \leftrightarrow N_2O_4$ the equilibrium constant in terms of the partial pressure corresponding to each species is [31]:

$$K_P = \frac{P_{NO_2}^2}{P_{NO_4}}$$

(5)

For pure $NO_2$ Eq. (5) can be written as:

$$K_P = \frac{P_{NO_2}^2}{P_T - P_{NO_2}}$$

(6)

where $P_T = P_{NO_2} + P_{N_2O_4}$

**Table 5**
Peak position of the IR bands of a frozen $NO_2: N_2O_4 = 1: 1$ mixture as deposited and their assignment. When two species compete for the same spectral feature we use the slash symbol to consider both of them. The slash is also used for the identification of the vibrational modes and references, respectively.

| Wavenumber ($cm^{-1}$) | Mode | Molecules | References |
|---|---|---|---|
| 1262 | $\nu_{11}$ | $N_2O_4$ | [32–35] |
| 1279 | $\nu_{11} + R^*$ | $N_2O_4$ | [32,33] |
| 1304 | $\nu_1/\nu_1$ | $NO_2/N_2O$ | [36]/[22,29,30] |
| 1613 | $\nu_3$ | $NO_2$ | [32,36] |
| 1720 | $\nu_7$ | $N_2O_4$ | [32,35] |
| 1741 | $\nu_9$ | $N_2O_4$ | [32–35] |
| 1765 | $\nu_9 + R^*/\nu_6 + \nu_{11}$ | $N_2O_4$ | [32,33]/[34] |
| 1860 | $\nu_4 + \nu_5/\nu_1$ | $N_2O_4/NO$ | [33]/[25] |
| 2235 | $\nu_3$ | $N_2O$ | [22,29,30] |
| 2328 | $\nu_1$ | $N_2$ | [37] |
| 2346 | $\nu_3$ | $CO_2$ | [38] |
| 2599 | $\nu_1 + \nu_{11}/2\nu_1$ | $N_2O_4/N_2O$ | [33]/[22,29,30] |
| 2638 | $2\nu_7 + \nu_{11}$ | $N_2O_4$ | [33] |

$^*$ $R$ = torsional lattice vibrations.
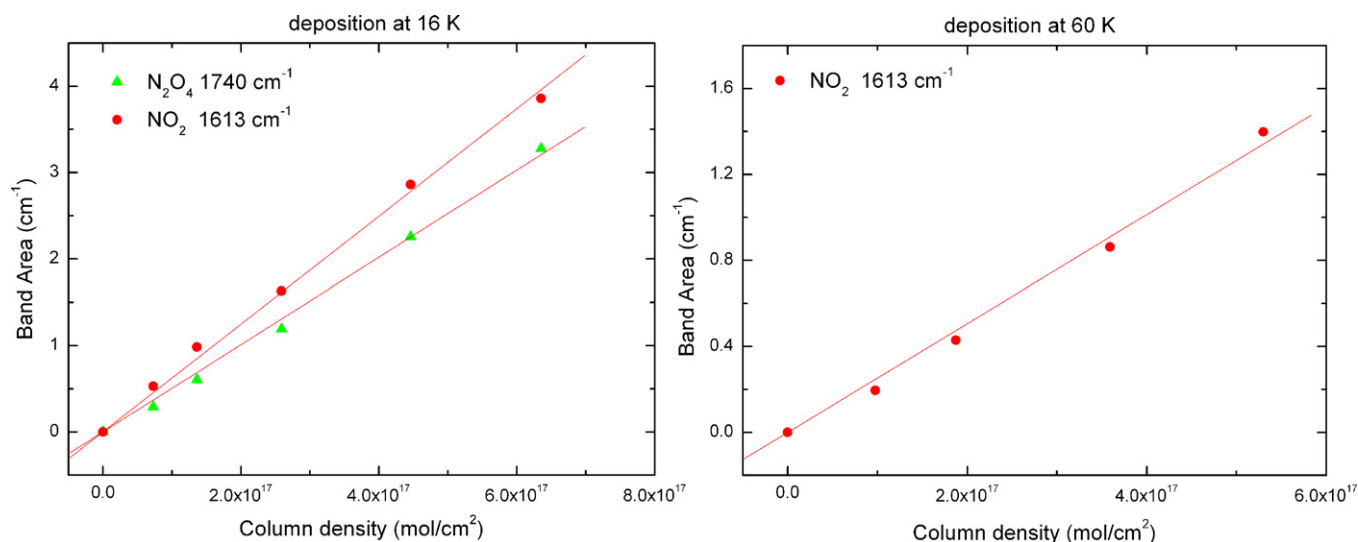
**Fig. 7.** Plot of the band area vs. the column density for the $NO_2$ band at 1613 cm$^{-1}$ and for the $N_2O_4$ band at 1740 cm$^{-1}$. The slope of the fit (solid line) gives the value of the integrated band strength A for the corresponding band (see Table 6).

Since the value of the $K_P$ constant is 104 mbar at 294 K [31] and the total pressure in the pre-chamber is 100 mbar, by means of Eq. (6) we can calculate the partial pressure of $NO_2$ and $N_2O_4$ in the gas phase under the given conditions. The values of partial pressure calculated in this way give a mixture $NO_2$:$N_2O_4$ = 1:1 and we assume the same relative concentration of $NO_2$ and $N_2O_4$ even for the deposited solid phase. In this work we performed experiments at two different deposition temperatures: 16 and 60 K. Figs. 5 and 6 show the IR spectra of two $NO_2$:$N_2O_4$ = 1:1 mixtures deposited respectively at 16 K and at 60 K on a Si substrate, again in an optical depth scale.

For the correct interpretation of Figs. 5 and 6, we should keep in mind that $N_2O_4$ is a molecule that presents both stable and metastable molecular configurations. The presence, shape and peak position of the bands associated with the $N_2O_4$ metastable structures are strongly related to the deposition rate and substrate temperature [32]. From these figures it is also evident that the profile of the main absorption bands for both $NO_2$ monomer and stable $N_2O_4$ dimer (for their identification see Table 5 and references therein) depends on the structure of the species constituting the frozen mixture, on their mobility and the relative amounts of each species. Moreover, in these spectra we can see the presence of additional bands which are attributed to $N_2O$, NO, $N_2$ and $CO_2$. We think that these species are contaminants present in the lecture bottle, since these are not observed in the spectra of other samples, such as the $N_2O$ spectra shown in Fig. 3.

Fig. 7 shows the plots of the band area against the column density. The best-fit of these data was used to derive the A values for the $NO_2$ band at 1613 cm$^{-1}$ at both 16 and 60 K. For the $N_2O_4$ band at 1740 cm$^{-1}$ the A value is derived only at 16 K, because in the case of the frozen mixture at 60 K, to measure the area of this band, we should take into account the strong and not quantifiable contribution (see Fig. 6) from the contiguous band at 1765 cm$^{-1}$.

In the A value computation we considered five increasing film thicknesses (up to 1.051 μm) for each band. Table 6 reports the integrated band strength values so estimated.

## 4. Final remarks

N–O bearing molecules are very important in both astrophysical and Earth's atmosphere sciences. However, there are a number of unsolved question regarding the N–O bearing species found in the gas phase in astrophysical sources (only NO, HNO and $N_2O$) and the lack of detection of N–O bearing molecules in the solid phase in interstellar frozen grain mantles. Another unsolved question regards the possibility of detecting these molecules in some bodies of the outer Solar System such as Pluto and Triton. In fact, near-infrared observations have already revealed the presence of $N_2$ and CO in the solid phase on their surface so, taking into account the chemical alterations induced by solar wind ions, solar UV photons and galactic cosmic rays on their molecular bonds, we can expect to detect N–O bearing species even in these objects because of ion and/or UV processing [22].

Conscious of the above mentioned importance of the N–O bearing molecules, in this paper we have presented novel measurements of the integrated band strengths of mid-infrared features for solid $N_2O$ at 16 K and for $NO_2$ and $N_2O_4$ in two frozen $NO_2$:$N_2O_4$ mixtures deposited at 16 and 60 K, respectively. The measurements reported will allow us to calculate the abundances of these molecules from observed mid-infrared spectra in both the astrophysical and terrestrial environments above mentioned. Moreover, refractive index and density measurements are given for solid $N_2O$ at 16 K, frozen $NO_2$:$N_2O_4$ mixtures deposited at 16 and 60 K and frozen $O_2$ at 16 K. For the last species the integrated band strength values have not been determined since $O_2$ is an homonuclear molecule.

**Table 6**
Peak positions and integrated band strengths for the two most intense features respectively of $NO_2$ and $N_2O_4$ deposited at 16 and 60 K on a Si substrate.

| Species – Peak position | Temperature | |
|---|---|---|
| | 16 K<br>A (cm molecule$^{-1}$) | 60 K<br>A (cm molecule$^{-1}$) |
| $NO_2$ – 1613 cm$^{-1}$ | $6.24 \times 10^{-18}$ | $2.53 \times 10^{-18}$ |
| $N_2O_4$ – 1741 cm$^{-1}$ | $5.05 \times 10^{-18}$ | – |

# References

[1] D. McGonagle, W.M. Irvine, Y. Minh, L.M. Ziurys, ApJ 359 (1990) 121–124.
[2] L.M. Ziurys, D. McGonagle, Y. Minh, W.M. Irvine, ApJ 373 (1991) 535–542.
[3] L.M. Ziurys, J.M. Hollis, L.E. Snyder, ApJ 430 (1994) 706–712.
[4] L.M. Ziurys, A.J. Apponi, J.M. Hollis, L.E. Snyder, ApJ 436 (1994) L181–L184.
[5] D.T. Halfen, A.J. Apponi, L.M. Ziurys, ApJ 561 (2001) 244–253.
[6] D.C.B. Whittet, M.F. Bode, A.J. Longmore, A.J. Adamson, A.D. McFadzean, D.K. Aitken, P.F. Roche, MNRAS 233 (1988) 321–336.
[7] A.G.G.M. Tielens, A.T. Tokunaga, T.R. Geballe, F. Baas, ApJ 381 (1991) 181–199.
[8] E.L. Gibb, D.C.B. Whittet, A.C.A. Boogert, A.G.G.M. Tielens, ApJ SS 151 (2004) 35.
[9] M.E. Palumbo, G. Strazzulla, Astron. Astrophys. 269 (1993) 568–580.
[10] K. Demyk, E. Dartois, L. D'Hendecourt, M. Jourdain de Muizon, A.M. Heras, M. Breitfellner, Astron. Astrophys. 339 (1998) 553–560.
[11] M.J. Loeffler, G.A. Baratta, M.E. Palumbo, G. Strazzulla, R.A. Baragiola, Astron. Astrophys. 435 (2005) 587–594.
[12] R.H. Brown, D.P. Cruikshank, J. Veverka, P. Helfenstein, J. Eluszkiewicz, Neptune and Triton, University of Arizona Press, Tucson, 1995, pp. 991–1030.
[13] D.P. Cruikshank, R.H. Brown, W.M. Calvin, T.L. Roush, M.J. Bartholomew, Solar System Ices, vol. 227, ASSL Series, Dordrecht, 1995, p. 579.
[14] G. Strazzulla, R.E. Johnson, Comets in the post-Halley Era, 1, ASSL Series, Dordrecht, 1991, 243–275.
[15] M.H. Moore, R.L. Hudson, Icarus 161 (2003) 486–500.
[16] B. Vandenbussche, P. Ehrenfreund, A.C.A. Boogert, E.F. van Dishoeck, W.A. Schutte, P.A. Gerakines, J. Chiar, A.G.G.M. Tielens, J. Keane, D.C.B. Whittet, M. Breitfellner, M. Burgdorf, Astron. Astrophys. 346 (1999) L57–L60.
[17] W.M. Calvin, R.N. Clark, R.H. Brown, J.R. Spencer, J. Geophys. Res. 100 (1995), 14091–14048.
[18] J.R. Noxon, Science 189 (1975) 547–549.
[19] G.E. Shaw, J. Geophys. Res. 81 (1976) 5791–5792.
[20] B.J. Finlayson-Pitts, J.N. Pitts Jr., Chemistry of the Upper and Lower Atmosphere, Academic, San Diego, 2000, pp. 264–277.
[21] M. Ackerman, J. Atm. Sci. 32 (1975) 1649–1657.
[22] B. Sivaraman, S. Ptasinska, S. Jheeta, N.J. Mason, Chem. Phys. Lett. 460 (2008) 108–111.
[23] G.A. Baratta, M.E. Palumbo, J. Opt. Soc. Am. A 15 (1998) 3076–3085.
[24] B.E. Wood, J.A. Roux, J. Opt. Soc. Am. 72 (1982) 720–728.
[25] J.A. Roux, B.E. Wood, A.M. Smith, R.R. Plyler, Arnold Engineering Development Center Report, AEDC-TR-79–81, 1980.
[26] M.S. Westley, G.A. Baratta, R.A. Baragiola, J. Chem. Phys. 108 (1998) 3321–3326.
[27] M.E. Palumbo, G.A. Baratta, M.P. Collings, M.R.S. McCoustra, Phys. Chem. Chem. Phys. 8 (2006) 279–284.
[28] G.A. Baratta, M.E. Palumbo, G. Strazzulla, Astron. Astrophys. 357 (2000) 1045–1050.
[29] D.A. Dows, J. Chem. Phys. 26 (1957) 745–747.
[30] A. Lapinski, J. Spanget-Larsen, J. Waluk, J.G. Radziszewski, J. Chem. Phys. 115 (2001) 1757–1764.
[31] A.C. Vandaele, C. Hermans, S. Fally, M. Carleer, R. Colin, M.-F. Mérienne, A. Jenouvrier, B. Coquart, J. Geophys. Res. D 107 (2002) CiteID 4348, doi:10.1029/2001JD000971.
[32] W.G. Fateley, H.A. Bent, B. Crawford Jr., J. Chem. Phys. 31 (1959) 204–217.
[33] R.N. Wiener, E.N. Nixon, J. Chem. Phys. 26 (1957) 906–908.
[34] B. Andrews, A. Anderson, J. Chem. Phys. 74 (1981) 1534–1537.
[35] I.C. Hisazune, J.P. Devlin, Y. Wada, J. Chem. Phys. 33 (1960) 714–719.
[36] T. Shimanouchi, J. Phys. Chem. Ref. Data 6 3 (1972) 993–1102.
[37] M.P. Bernstein, S.A. Sandford, Spectrochim. Acta A 55 (1999) 2455–2466.
[38] S.A. Sandford, L.J. Allamandola, ApJ 355 (1990) 357–372.